AN EXPERIMENTAL STUDY OF SEVERAL WIND TUNNEL WALL CONFIGURATIONS USING TWO V/STOL MODEL CONFIGURATIONS

T. W. Binion, Jr.

Arnold Engineering Development Center

Prepared for:

ARO, Incorporated
National Aeronautics and Space Administration

July 1975

AEDC-TR-75-58

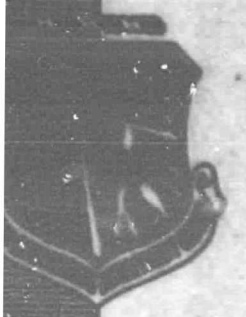

AN EXPERIMENTAL STUDY OF SEVERAL WIND TUNNEL WALL CONFIGURATIONS USING TWO V/STOL MODEL CONFIGURATIONS

PROPULSION WIND TUNNEL FACILITY
ARNOLD ENGINEERING DEVELOPMENT CENTER
AIR FORCE SYSTEMS COMMAND
ARNOLD AIR FORCE STATION, TENNESSEE 37389

July 1975

Final Report for Period March 1972 – April 1974

Prepared for

AMES RESEARCH CENTER
NATIONAL AERONAUTICS AND SPACE ADMINISTRATION
MOFFETT FIELD, CALIFORNIA 94035

REPORT DOCUMENTATION PAGE	READ INSTRUCTIONS BEFORE COMPLETING FORM
1 REPORT NUMBER: AEDC-TR-75-36	2 GOVT ACCESSION NO. / 3 RECIPIENT'S CATALOG NUMBER
4 TITLE (and Subtitle): AN EXPERIMENTAL STUDY OF SEVERAL WIND TUNNEL WALL CONFIGURATIONS USING TWO V/STOL MODEL CONFIGURATIONS	5 TYPE OF REPORT & PERIOD COVERED: Final Report - March 1972 - April 1974
	6 PERFORMING ORG. REPORT NUMBER
7 AUTHOR(s): T. W. Binion, Jr., ARO, Inc.	8 CONTRACT OR GRANT NUMBER(s)
9 PERFORMING ORGANIZATION NAME AND ADDRESS: Arnold Engineering Development Center (XO) Air Force Systems Command Arnold Air Force Station, TN 37389	10 PROGRAM ELEMENT, PROJECT, TASK AREA & WORK UNIT NUMBERS: Program Element 921E
11 CONTROLLING OFFICE NAME AND ADDRESS: Arnold Engineering Development Center (DYFS), Arnold Air Force Station, Tennessee 37389	12 REPORT DATE: July 1975
	13 NUMBER OF PAGES: 37
14 MONITORING AGENCY NAME & ADDRESS (if different from Controlling Office)	15 SECURITY CLASS. (of this report): UNCLASSIFIED
	15a DECLASSIFICATION DOWNGRADING SCHEDULE: N/A

16 DISTRIBUTION STATEMENT (of this Report)

Approved for public release; distribution unlimited.

17 DISTRIBUTION STATEMENT (of the abstract entered in Block 20, if different from Report)

18 SUPPLEMENTARY NOTES

Available in DDC

19 KEY WORDS (Continue on reverse side if necessary and identify by block number)

wind tunnels
walls
wall interference
vertical takeoff aircraft
short takeoff aircraft
jet flaps

20 ABSTRACT (Continue on reverse side if necessary and identify by block number)

Experiments were conducted in the AEDC Low Speed Wind Tunnel (V/STOL), Propulsion Wind Tunnel Facility (PWT), with two V/STOL models, a jet-flap and a jet-in-fuselage configuration, to search for a wind tunnel wall configuration to minimize wall interference on V/STOL models. Data were also obtained with the jet-flap model and a uniform slotted wall configuration to provide comparisons between theoretical and experimental wall interference. A test

DD FORM 1 JAN 73 1473 EDITION OF 1 NOV 65 IS OBSOLETE

PRICES SUBJECT TO CHANGE

20. ABSTRACT (Continued)

section configuration was found which for the jet-flap model yields data in reasonable agreement with interference-free results over a wide range of momentum coefficients. However, the configuration does not yield interference-free data for the jet-in-fuselage model. The key to development of an interference-free wall configuration for V/STOL models lies in the development of an understanding of the complex interaction between the downwash of the augmented lift device and the tunnel boundary. It is shown that agreement between wall interference theory and experiment for the V/STOL case can hinge upon the theoretical representation of the boundary condition.

PREFACE

The work presented herein was conducted by the Arnold Engineering Development Center (AEDC), Air Force Systems Command (AFSC), at the request of the Ames Research Center (ARC), National Aeronautics and Space Administration (NASA), under Program Element 921E. The results of the research were obtained by ARO, Inc. (a subsidiary of Sverdrup & Parcel and Associates, Inc.), contract operator of AEDC, AFSC, Arnold Air Force Station, Tennessee. The work was conducted under ARO Project Nos. PW5214, PF211, and PF411. The author of this report was T. W. Binion, Jr., ARO, Inc. The research was conducted from March 10, 1972 to April 16, 1974, and the manuscript (ARO Control No. ARO-PWT-TR-75-4) was submitted for publication on January 20, 1975.

CONTENTS

ILLUSTRATIONS

Figure

1.0 INTRODUCTION

Aerodynamic data obtained from high-lift vertical or short takeoff and landing (V/STOL) vehicles in wind tunnels in many instances contain large interference effects caused by the constraints imposed by the tunnel boundaries. A practical solution for coping with the boundary interference is to develop a wall configuration which reduces the interference to acceptable levels. The fact that the interference produced by solid and open boundaries have opposite signs, Ref. 1, led early investigators, Ref. 2, to explore partially open boundaries as a means of reducing wall interference. Numerous investigations, summarized in Ref. 3, have led to the various ventilated test sections used in all parts of the world today. The test sections which have evolved are, however, designed to reduce the wall interference associated with conventional aerodynamic vehicles primarily in the transonic speed range.

There seems to be no inherent reason why the ventilated wall concept cannot be applied to relieve wind tunnel wall interference associated with V/STOL models. The initial effort toward the development of such a wall configuration, Ref. 4, used a high-disc-loading jet-in-fuselage model as the stream disturbing device. The results of that program indicated the probability that a minimal-interference wall could be devised. The work reported herein is an extension of that reported in Ref. 4 to consider additional wall configurations with the jet-in-fuselage model and to explore the effect of model configurations by also testing with a jet-flap model. Chronologically, wall configurations were tested with the jet-in-fuselage model until one was found which produced reasonably interference-free results for a wide range of model jet to tunnel velocity ratios. The jet-flap model was then installed and 47 additional wall modifications were tested. The minimal-interference configuration thus evolved was then tested with the jet-in-fuselage model to determine if the wall configuration was also suitable for testing high-disc-loading models.

Force and moment data were obtained on the jet-in-fuselage model in the 7- by 10-ft test section of the Ling-Temco-Vought (LTV) Low Speed Wind Tunnel and on the jet-flap model in the NASA Ames 40- by 80-ft Subsonic Wind Tunnel. These data, considered to be interference free, were used to evaluate the wall interference by comparison with data obtained with various wall configurations in the 30- by 45-in. test section of the AEDC Low Speed Wind Tunnel (V/STOL).

Tests with the jet-in-fuselage model in the V/STOL tunnel were limited to a jet-to-free-stream velocity ratio of 4.5 which is just below the condition of complete flow breakdown as defined in Ref. 5. Tests with the jet flap were limited to a momentum coefficient of 3.3 which corresponds to a sonic jet at a tunnel dynamic pressure of 2 psf.

2.0 APPARATUS

2.1 WIND TUNNELS

Data on the jet-flap model, which are considered interference free, were obtained in the NASA/Ames 40- by 80-ft Subsonic Wind Tunnel. The 40- by 80-ft tunnel is a continuous flow, atmospheric pressure, closed-throat, closed-circuit facility. The speed range is continuously variable from zero to 200 knots. A description of the facility may be found in Ref. 6.

Data on the jet-in-fuselage model which are considered interference free were obtained in the LTV Low Speed Wind Tunnel. The LTV tunnel is a continuous flow, atmospheric pressure, single return, closed-throat system. The rectangular 15- by 20-ft test section is followed by a 7- by 10-ft test section with speed ranges of 12 to 60 ft/sec and 80 to 320 ft/sec, respectively. A complete description of the tunnel, its operating characteristics, and associated equipment are contained in Ref. 7.

The wall interference study was conducted in the AEDC Low Speed Wind Tunnel (V/STOL). The V/STOL tunnel is a continuous flow, closed-circuit, atmospheric pressure test unit in which speeds from 5 to 220 ft/sec can be obtained. The test section has a 30- by 45-in. cross section and is 72 in. long. The test section walls may be independently modified to allow a wide variety of wall configurations to be used. The test section is enclosed in a 9- by 9-ft sealed plenum which allows a constant free-stream static pressure environment to be maintained around the test section. A complete description of the tunnel, its operating characteristics, and associated equipment are presented in Ref. 8.

2.2 MODELS

2.2.1 Jet Flap

The jet-flap model, shown installed in the V/STOL tunnel in Fig. 1a, consists of a hollow, rectangular, planform wing and a horizontal tail. The sting also serves as a model centerbody, air line, and instrumentation lead shield. The pertinent model dimensions are given in Fig. 2a.

Each wing contains a plenum chamber supplied with high-pressure nitrogen which exhausts through a 0.020-in. slit near the trailing edge to form the jet flap. The wing has an NACA 0012 airfoil truncated at 95-percent of the chord with a constant radius trailing edge. The left wing contains a specially designed five-component balance. The nitrogen supply passes symmetrically through the balance to eliminate the need to compensate for internal momentum changes. It was found necessary, however, to correct

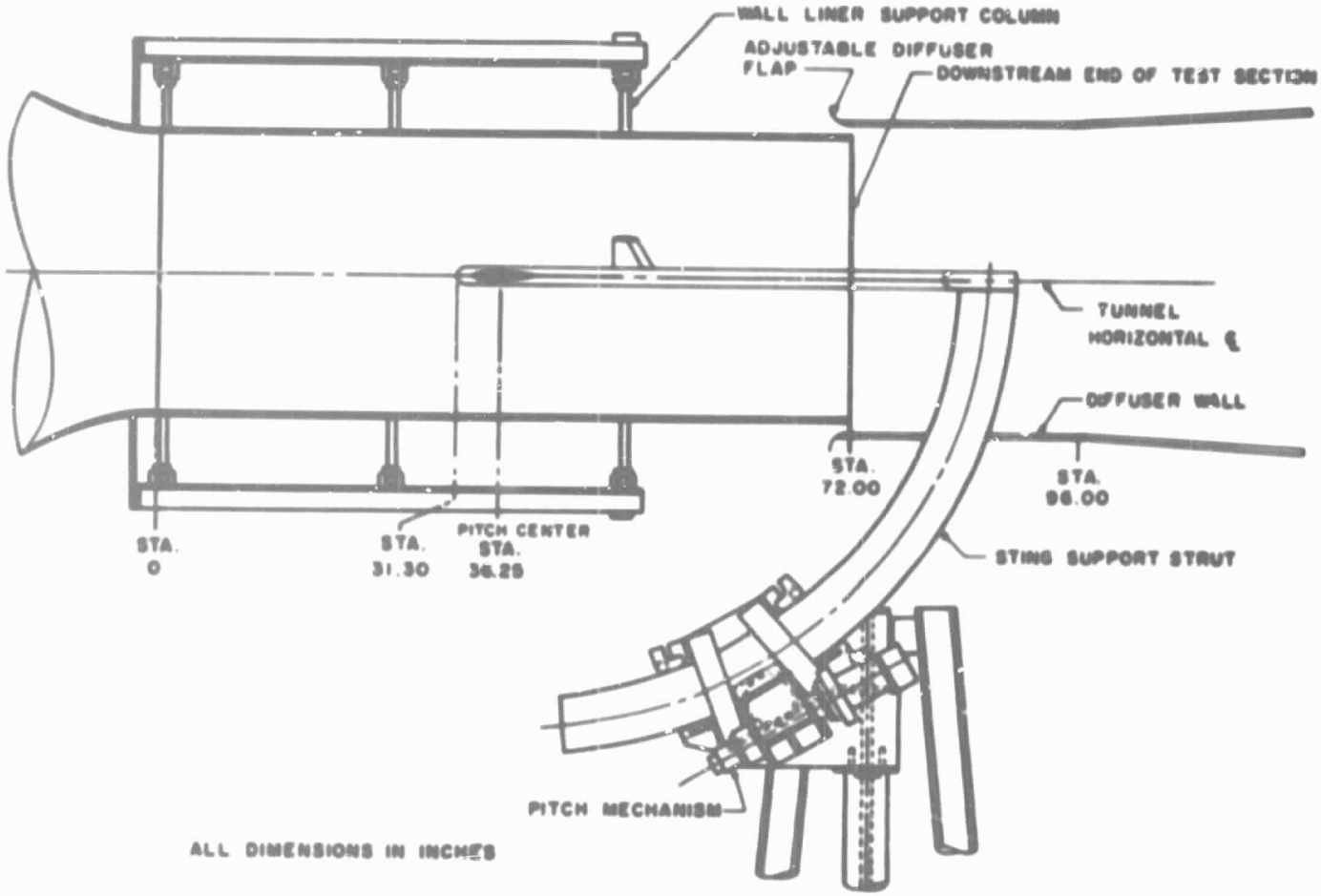

a. Jet-flap model

Figure 1. Model location in the V/STOL wind tunnel.

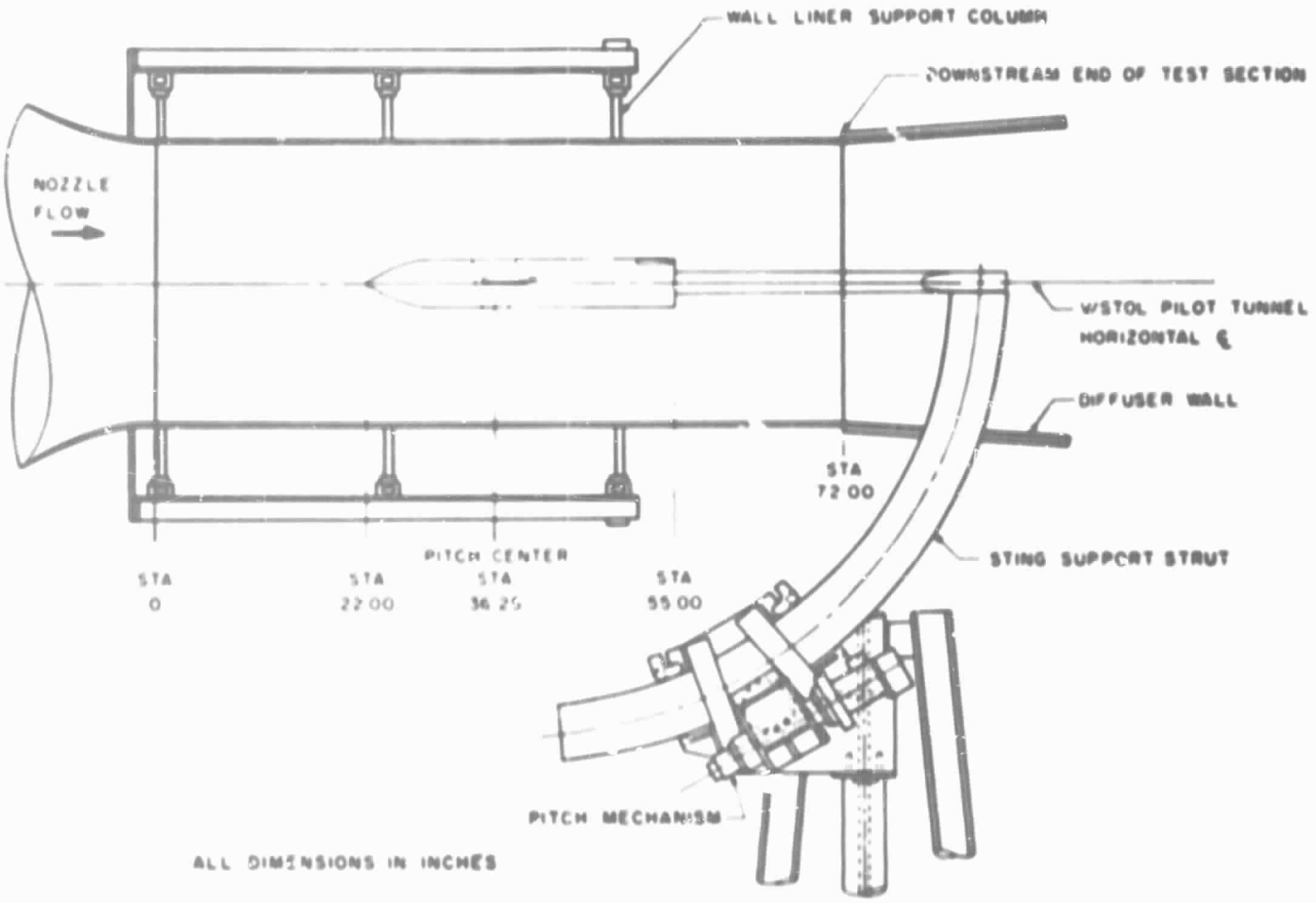

b. Jet-in-fuselage model

Figure 1. Concluded.

the balance readings to compensate for the effects of the internal pressure. The right wing contains an adjustable restriction which is used to balance the flow in the two wings. The horizontal tail, also utilizing an NACA 0012 airfoil, is mounted on a two-component balance which is shielded by the vertical fairing.

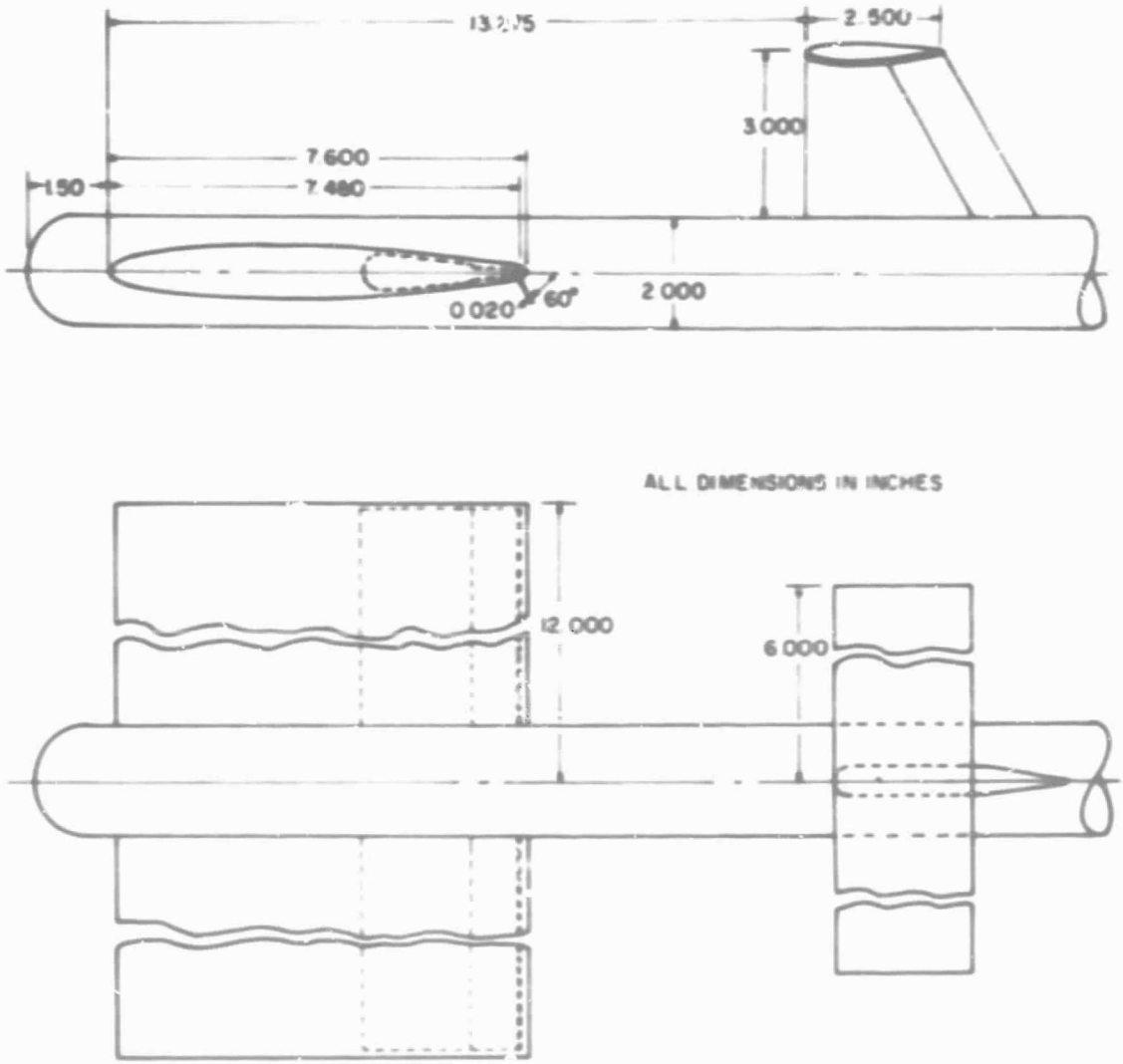

a. Jet-flap model

Figure 2. Model dimensions.

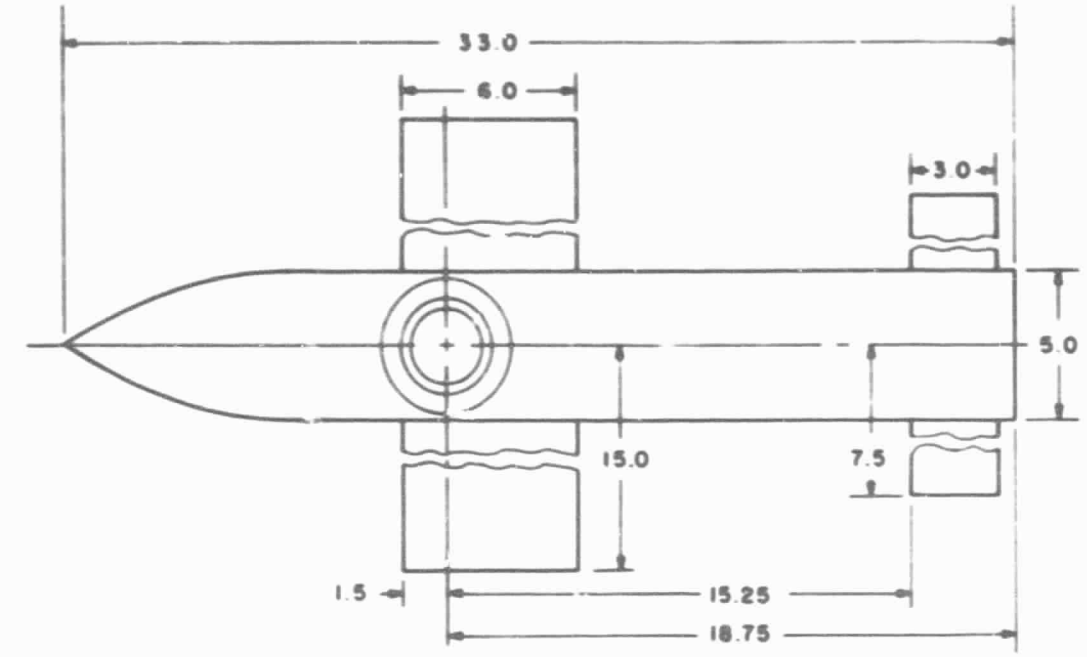

ALL DIMENSIONS IN INCHES

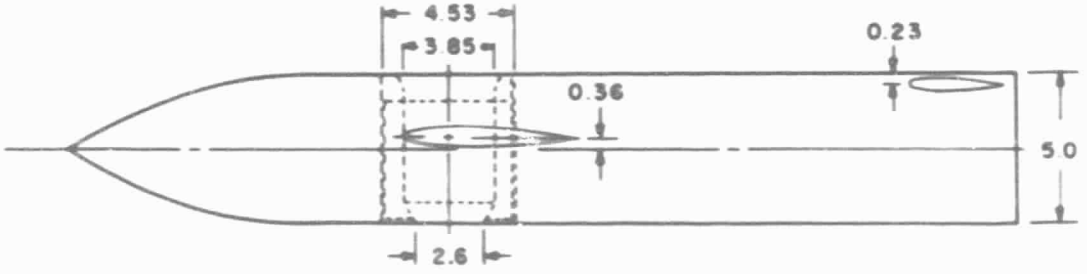

b. Jet-in-fuselage model
Figure 2. Concluded.

2.2.2 Jet-in-Fuselage Model

The jet-in-fuselage model, shown installed in the V/STOL tunnel in Fig. 1b, consists of an air ejector surrounded by a minimum cross-sectional area fuselage, a mid-fuselage wing, and a removable horizontal tail. The air ejector and its inlet are mechanically separated from the fuselage by a labyrinth seal. High-pressure nitrogen was supplied to the ejector through the sting. The fuselage has a square cross section with corners rounded of a 0.25 in. radius. Both the wing and tail have an NACA 0012 airfoil section. The pertinent model dimensions are given in Fig. 2b.

The model contains two strain-gage balances. One measures the normal force of the ejector and its inlet. The other measures the normal force, axial force, and pitching moment of the wing-fuselage-tail assembly. Thus, the ejector forces are measured separately from the aerodynamic forces on the model.

2.3 WALL CONFIGURATIONS

Data were obtained with two basic wall configurations. The first, which was tested to obtain data for comparison with theory, had ten equally spaced, constant width slots in each horizontal wall and solid sidewalls. The slot width was varied from zero to 1 in. resulting in a wall porosity variation from zero to 22.2 percent.

The second basic test section configuration, shown in Fig. 3, consisted of solid side walls, a slotted upper wall, a louvered lower wall (Fig. 4), and independent upper and lower plena. The following geometric parameters were varied: upper and lower slot width, a_u and a_L, upper and lower plenum depth, D_u and D_L, lower wall louver angle, θ, lower wall step location, L, and the lower wall louver step height, s. In addition, with $D_L \leq 8$ in., it was found necessary to supply tunnel air to the lower plenum so that a small mass flow passed through the rearward facing step into the test region. This was accomplished by a transverse slot of width g at the nozzle exit.

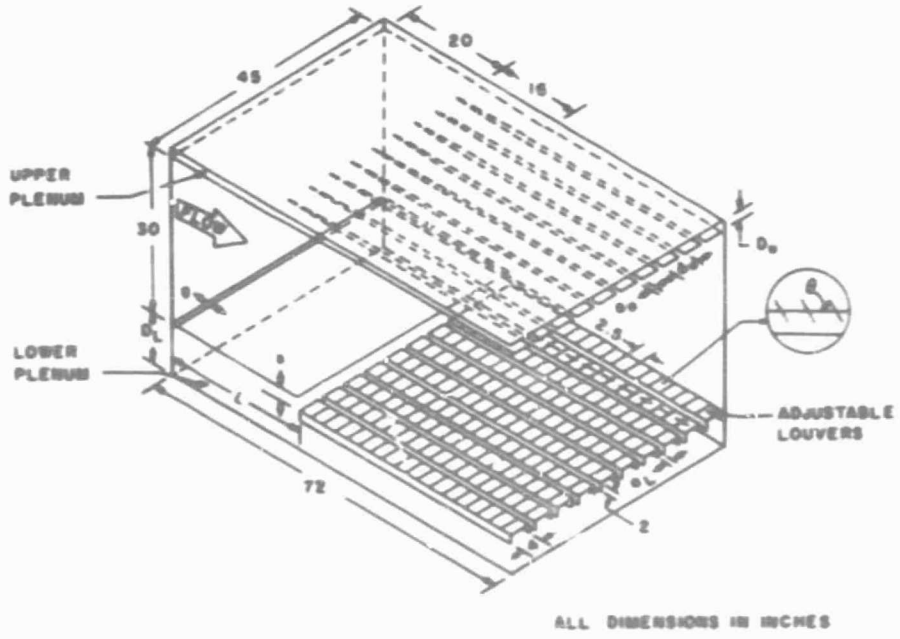

Figure 3. Basic stepped configuration.

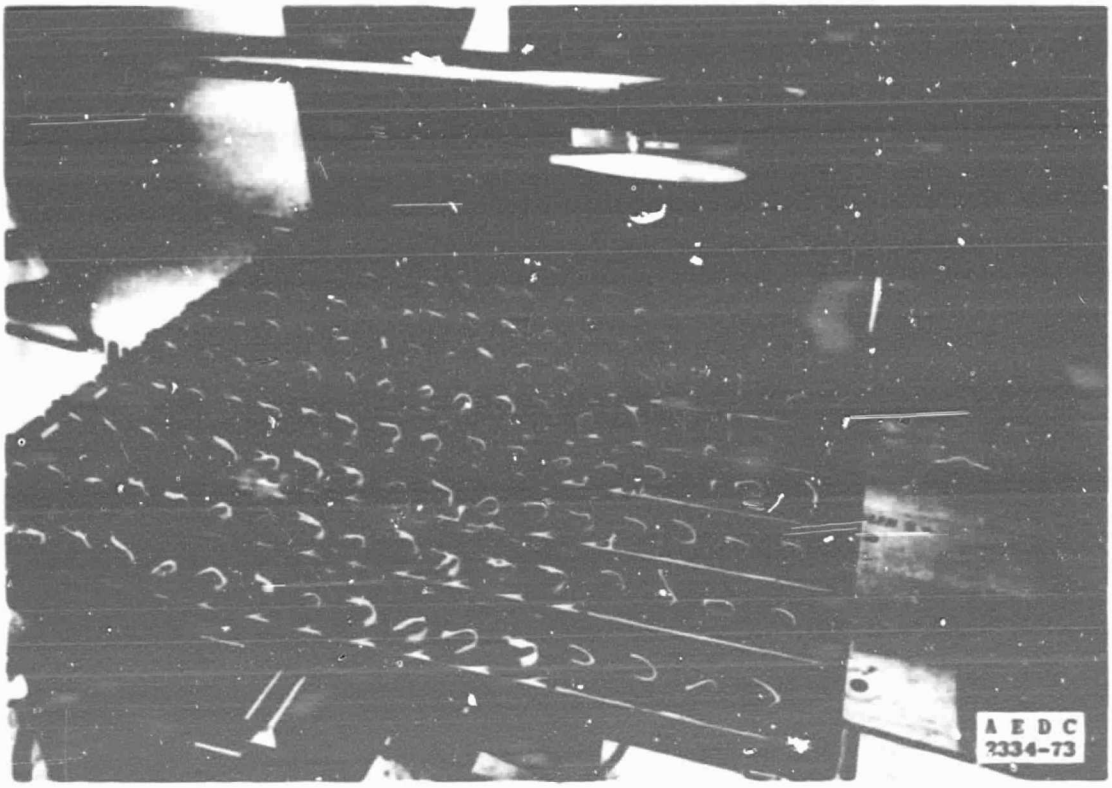

Figure 4. Louvered bottom test section wall.

2.4 INSTRUMENTATION

Model forces and moments were obtained from strain gages placed on specially designed balance beams internal to the models. The tunnel nozzle-exit pressure, which was used as a reference for all other pressure measurements, was measured with a precision, servo-driven, mercury manometer. Other model and tunnel pressures were measured with strain-gage differential pressure transducers. Model and tunnel temperatures were measured with iron-constantan thermocouples. The instrumentation readings were recorded by an on-line computer system which reduced the raw data to engineering units, computed pertinent parameters, and tabulated the results.

3.0 PROCEDURE

3.1 TEST CONDITIONS AND PROCEDURES

3.1.1 Jet-Flap Model

Data were obtained in the AEDC V/STOL tunnel and the NASA Ames 40- by 80-ft tunnel at the same value of the jet momentum coefficient. In addition, because of a sizable

difference in the jet total temperature in the two facilities, it was found necessary to also test at the same values of jet momentum rather than jet total pressure. There was no control of the jet total temperature in either facility. The desired value of jet momentum was set by allowing the system to operate until near thermal equilibrium conditions were established and then adjusting the jet stagnation pressure until the desired value of jet momentum was achieved. The tunnel velocity was then adjusted to obtain the desired momentum coefficient. In general, data were obtained at momentum coefficients of 0, 0.05, 0.31, 0.94, 2.1, 2.8, and 3.3 for each tunnel wall configuration.

3.1.2 Jet-in-Fuselage Model

Data in the AEDC V/STOL tunnel and the LTV Low Speed Wind Tunnel were obtained at jet-to-free-stream velocity ratios of 0, 2.0, 3.3, and 4.5 with the horizontal tail off and on. The tunnel velocity was set to the desired value. High-pressure nitrogen was supplied to the ejector until the desired jet exit total pressure was obtained. The jet exit temperature was uncontrollable. No adjustment was made for its variation, however, since the aerodynamic forces were not significantly affected by small changes in the jet velocity for the selected free-stream conditions.

3.2 PRECISION OF THE DATA

The data contained herein were obtained from single-sample measurements. Uncertainties in the measured parameters were estimated from repeat calibrations of the instrumention. The uncertainties were combined using the Taylor series of error propagation to determine the precision of the reduced parameters presented below.

Jet-Flap Model

C_μ	ΔC_μ	ΔC_L	ΔC_{m_w}	ΔC_{L_T}
0	0	0.0013	0.0006	0.0025
0.05	0.0003	0.0021	0.0007	0.0021
0.30	0.003	0.0065	0.017	0.0051
0.94	0.015	0.0338	0.013	0.016
2.0	0.060	0.117	0.053	0.031
2.8	0.103	0.185	0.078	0.042
3.3	0.134	0.254	0.149	0.048

Jet-in-Fuselage Model

V_R	ΔV_R	ΔC_{L_f}	ΔC_{m_f}
0	0	0.011	0.005
2.0	0.01	0.009	0.005
3.3	0.03	0.017	0.008
4.5	0.04	0.022	0.008

The precision of the angle of attack is estimated to be 0.1 deg.

4.0 RESULTS AND DISCUSSION

4.1 COMPARISON OF EXPERIMENT AND THEORY

Although the primary objective of the investigation reported herein was to search for a minimal-interference wall configuration, data were taken with the jet-flap model and a series of ten constant width slots which could be described by theory. Theoretical solutions for the first order wall interference corrections are obtained by solving the field equation of an inviscid fluid in terms of the perturbation velocity potential ϕ, i.e.,

$$\left(\frac{\partial^2}{\partial x} + \frac{\partial^2}{\partial y} + \frac{\partial^2}{\partial z}\right)\phi = 0 \tag{1}$$

subject to the generalized homogeneous boundary condition

$$\frac{\partial \phi}{\partial x} + \frac{1}{R}\frac{\partial \phi}{\partial n} + k\frac{\partial^2 \phi}{\partial x \partial n} = 0 \tag{2}$$

Two expressions have been derived for the geometric slot parameters k, the earliest, originally derived by Gurdley, Ref. 9,

$$k_1 = \frac{\ell}{\pi} \ln \csc \frac{\pi}{2}\frac{a}{\ell} \tag{3}$$

and the second by Chen and Mears, Ref. 10, which neglecting the contribution of plate thickness can be written

$$k_2 = \frac{d - a}{2} \tan\left[\pi/2\left(1 - \frac{a}{d}\right)\right] \tag{4}$$

Kraft, Ref. 11, derived a quasi-linear slotted wall boundary condition for the walls normal to the lift vector given by

$$\frac{\partial \phi}{\partial x} + \frac{V_\infty}{U_\infty \cos \alpha_0}\frac{\partial \phi}{\partial z} + k\left(1 + \frac{V_\infty}{U_\infty \cos \alpha_0}\frac{\partial x}{\partial z}\right)\frac{\partial^2 \phi}{\partial x \partial z} = 0 \tag{5}$$

where V_e is the crossflow velocity at the boundary and α_o is the model incidence at zero lift. For the classical case, $V_e \approx 0$, Eq. (5) reduces to the common form of Eq. (2). For large values of V_e, Kraft shows that the second coefficient of Eq. (5) becomes a pseudoporosity parameter

$$\frac{1}{Re} = \frac{V_e}{u_\infty \cos \alpha_o} \tan \alpha_o \tag{6}$$

and the third coefficient becomes an effective slot parameter

$$k_e = 2k \tag{7}$$

where k is taken to be given by Eq. (4).

As shown in Ref. 4, the classical blockage and upwash interferences for a V/STOL model in a wind tunnel are coupled through the equations

$$U/U_\infty = \left[\left(1 + \delta_u \frac{s}{C} C_L\right)^2 + \left(\delta_w \frac{s}{C} C_L\right)^2\right]^{1/2} \tag{8}$$

$$\Delta\alpha = \frac{\delta_w \frac{s}{C} C_L}{1 + \delta_u \, s/C \, C_L} + \Delta\alpha_j \tag{9}$$

where U_∞ is the tunnel empty test section velocity, δ_u and δ_w are the interference factors derived from the axial and vertical perturbation velocities, respectively, and $\Delta\alpha_j$ is an angle-of-attack increment which is hypothesized to be required by wall induced changes in the jet trajectory. The term $\Delta\alpha_j$ can be evaluated experimentally at $C_L = 0$ by comparing interference and interference free C_L versus α data; however, no theoretical prediction of its existence, much less its behavior, is presently available. The interference factors δ_u and δ_w can be calculated by several available theoretical solutions, Refs. 11 through 13, for example. The experimental determination of δ_u and δ_w, however, requires either a third independent equation or a direct measurement of the velocity U, [Eq. (8)] which was not available during the present experiments. A theoretical estimate of the blockage effect for the jet-flap model in the V/STOL tunnel with solid walls shows the maximum value of U/U_∞ varies from 1.005 at $C_L = 1.0$ to 1.03 at $C_L = 6.0$. Thus, the error in assuming that the tunnel velocity is equal to the calibration velocity can be appreciable at high values of C_L, but the blockage effects can be reasonably neglected at values of C_L less than about two which corresponds to C_μ of about 0.9.

By assuming δ_u to be zero, experimental values of the upwash interference factors δ_w and $\Delta\alpha_j$ can be evaluated in the least squares sense by the method derived in Ref. 4.

The values of δ_w thus obtained are compared with theory in Fig. 5 for the three values of the wall boundary condition described above. The theoretical solutions were obtained by the method described in Ref. 14 using an elliptical wing loading and the boundary condition given by Eq. (5). The theoretical value of the upwash interference factor includes both the interference at the wing quarter chord position and the streamline curvature effect and is given by

$$\delta_w = \delta_o + \frac{\bar{c}}{4b} \cdot \frac{\partial \delta_w}{\partial x/b} \tag{10}$$

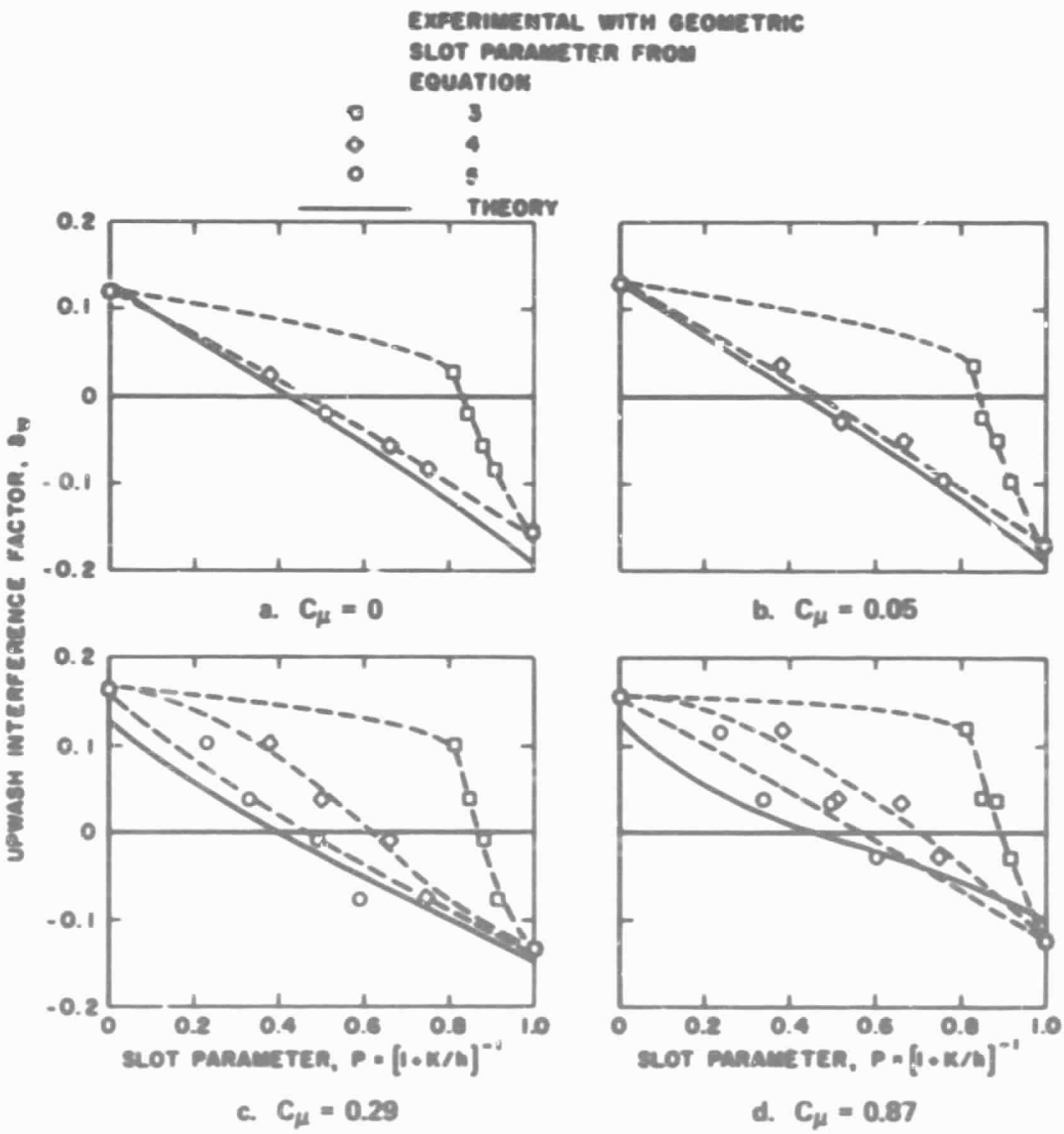

Figure 5. Comparison of experiment and theory.

The data in Fig. 5 show good agreement between theory and experiment at low values of C_μ when either Eq. (4) or (5), which are identities at low values of C_μ, is used. Although the data obtained at higher values of C_μ for the closed and open walls (P = 0 and 1, respectively) indicate possible blockage effects, which were thought to be minimal, the boundary condition given by Eq. (5) provides the best agreement between theory and experiment.

The variation of the jet interference parameter, Δa_j, presented in Fig. 6, is quite different from that obtained with the jet-in-fuselage model in Ref. 4. At a given value of the slot parameter, the value of Δa_j for the jet-in-fuselage model increased with increasing jet-to-free-stream velocity ratio. However, Δa_j for the jet-flap model, in general, decreases with increasing jet strength (increasing C_μ). Further, the data scatter is much greater with the jet-flap than with the jet-in-fuselage model. In both instances, however, for a constant value of jet strength, Δa_j decreases with increasing wall porosity. Also, the data with both models indicate a parameter of the form of Δa_j in Eq. (9) is required to correct the angle of attack to the free-air value. A very critical review of test procedures and techniques failed to reveal any item which could surreptitiously introduce the term. Thus, since Δa_j is a function of both jet strength and wall configuration, it is felt that Δa_j is the result of an interference phenomena whose nature remains to be identified.

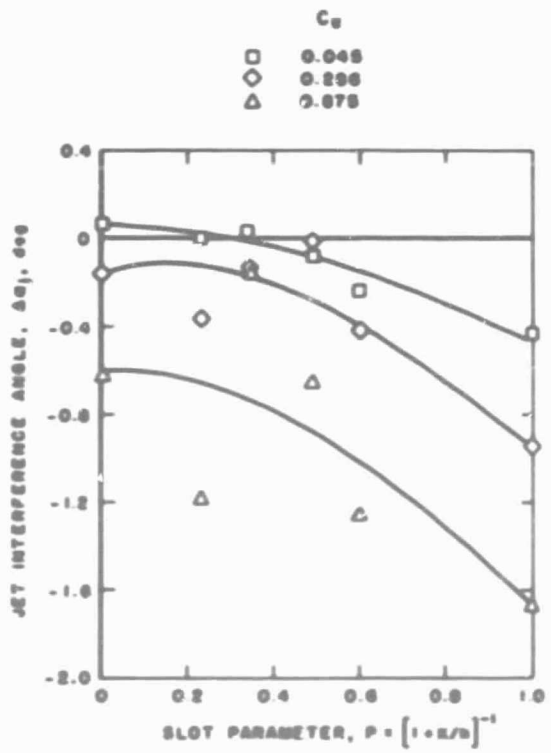

Figure 6. Jet interference angle with the uniform slotted wall configuration.

4.2 EVALUATION OF WALL CONFIGURATIONS WITH THE JET-FLAP MODEL

The final test section configuration evolved from a somewhat unsystematic parameter variation. If a given parameter had little effect upon the model forces and moments, particularly on C_{m_w}, the tunnel was not restored to its original configuration before the next parameter variation began. Thus, the parameter variations are not sufficiently detailed to allow the establishment of multidimensional influence coefficients. The data do, however, allow a number of effects to be shown over a limited range of parameter variations. It should be recognized that the data from the V/STOL tunnel contain the simultaneous influences of classical blockage and upwash interference, jet/boundary interactions, and in some instances possible intermittent test section flow separations. While these effects are not separable, they were in most cases very repeatable.

Seven force and moments were measured on the jet-flap model. The axial-force data obtained in the Ames 40- by 80-ft tunnel were apparently influenced by model support vibration in the axial direction causing erratic readings. Two moments, wing root bending caused by the normal and axial force, respectively, were not appreciably affected by the various wall configurations indicating that the spanwise loading is essentially unaffected by the interference phenomena. Thus, wall configuration evaluation is made on the basis of three aerodynamic coefficients, C_{L_w}, C_{m_w}, and C_{L_T}. It is assumed that if all model forces and moments obtained in the V/STOL tunnel are simultaneously in agreement with the large tunnel results, the flow field about the model approximates an interference-free field. The jet-flap model data are presented for two values of the momentum coefficient, which are representative of the results obtained at low and high values of C_μ.

The data obtained on the jet-flap model with solid test section walls and with the uniform slotted configuration are presented in Fig. 7 as a frame of reference for the subsequent stepped bottom wall configuration. At low C_μ, increasing the wall porosity decreases the slope of the C_L versus α data as expected. The wing pitching moment is only slightly affected. At high values of C_μ, however, not only is $\partial C_L / \partial \alpha$ decreased with increasing porosity but there is a large decrease in C_L for a given gravimetric angle of attack. Pitching moment is also substantially reduced. It was found that placing a step in the bottom wall favorably affected both the lift and pitching moment variation at high C_μ, as shown in Fig. 8, without appreciably affecting the data at low C_μ. It was also found that, as might be expected, the location of the step is an important parameter as shown in Fig. 9.

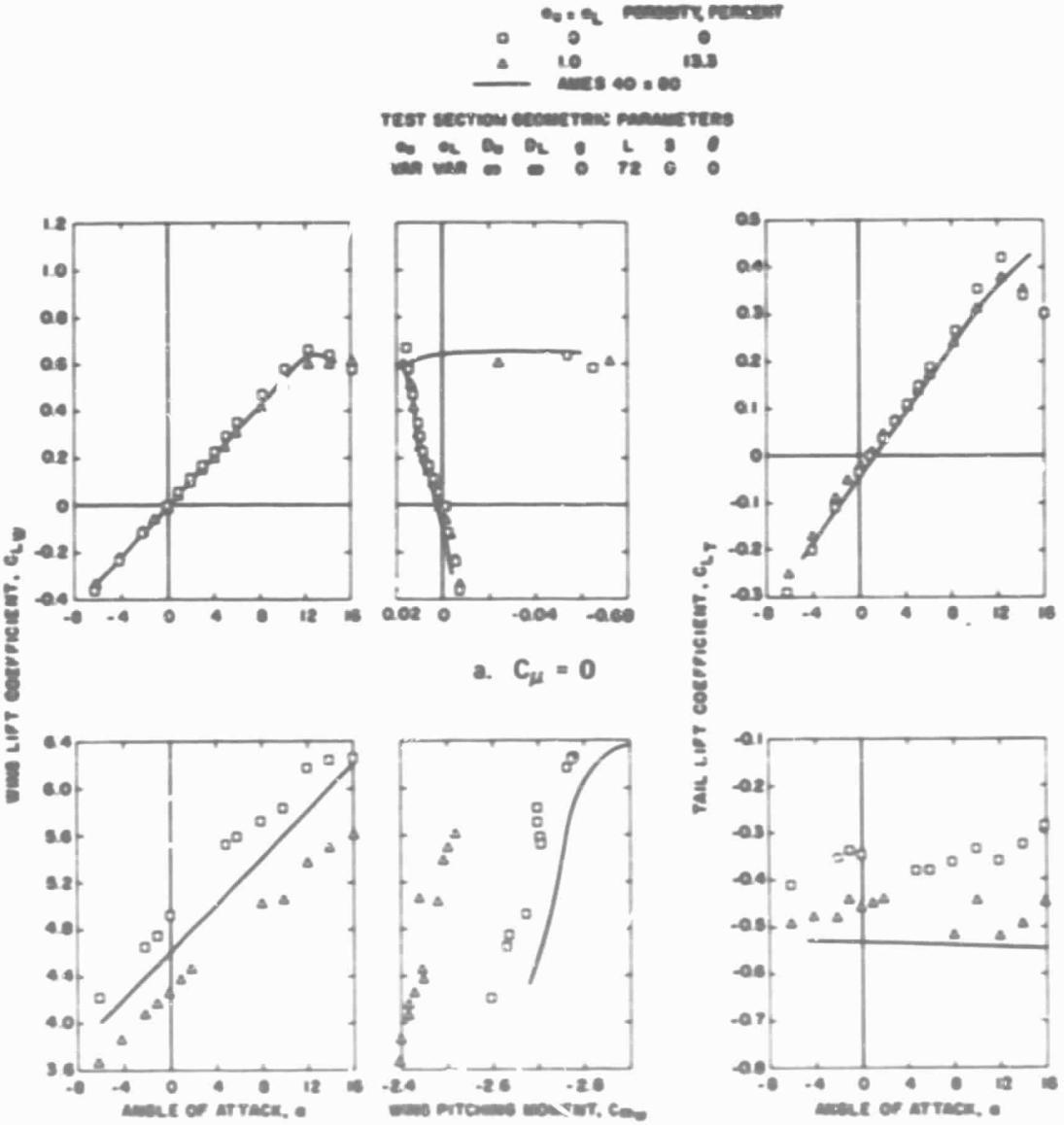

a. $C_\mu = 0$

b. $C_\mu = 3.3$

Figure 7. Interference on the jet-flap model with 10 uniform slots in each horizontal wall.

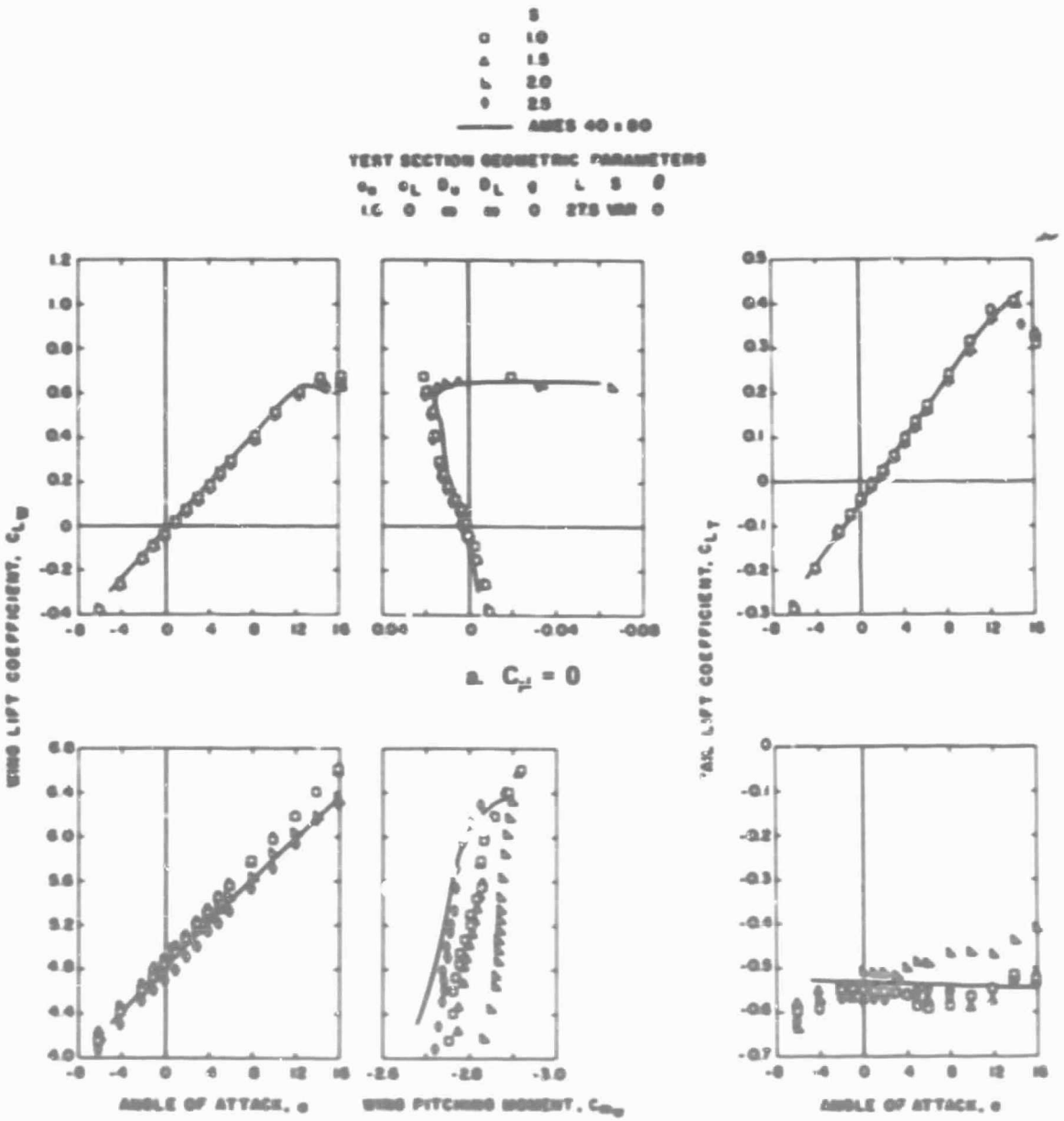

a. $C_\mu = 0$

b. $C_\mu = 3.3$

Figure 8. Effect of bottom wall step height on the jet-flap model forces.

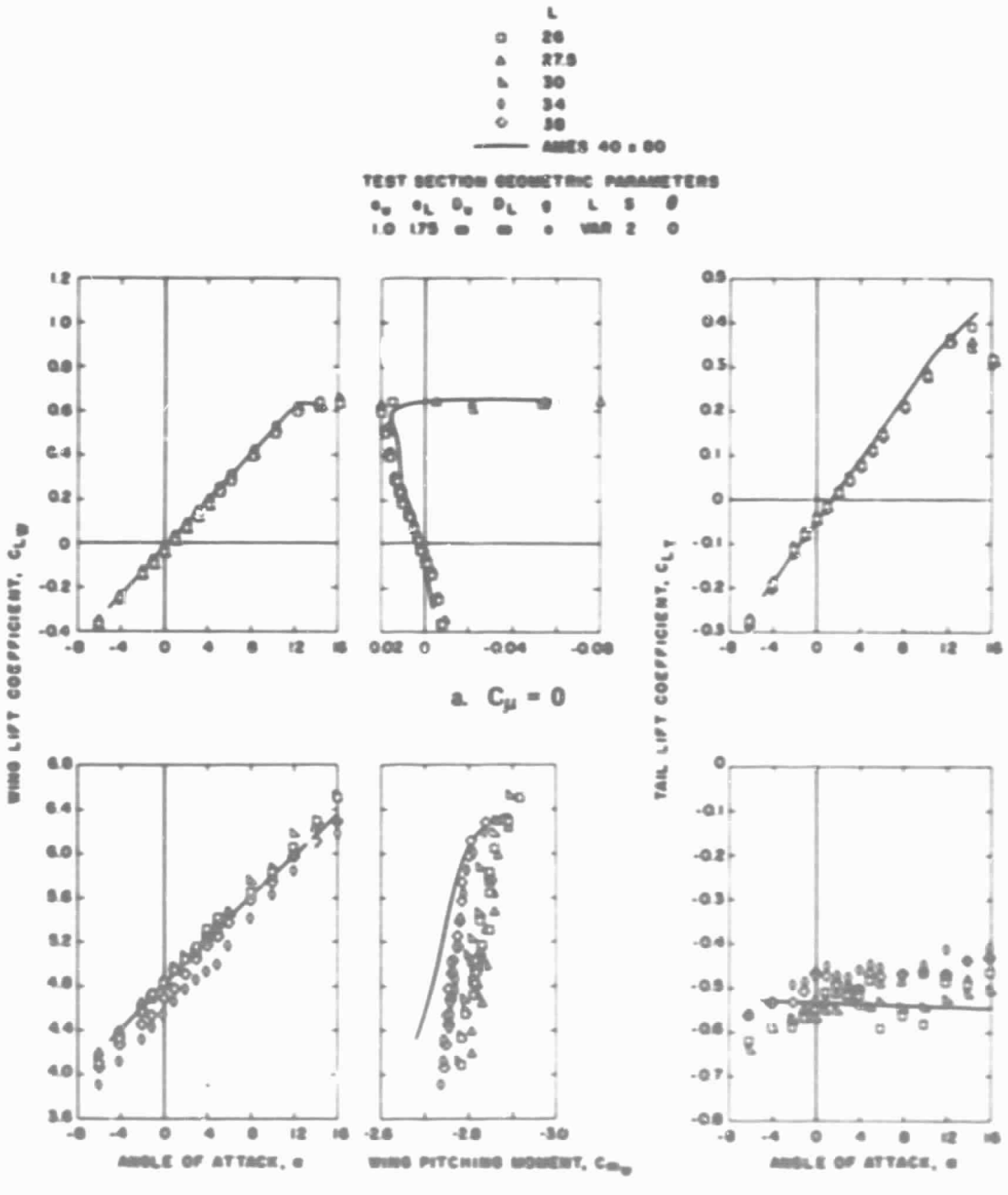

Figure 9. Effect of bottom wall step location on the jet-flap model forces.

Louvers in the bottom wall were conceived as a means of directing the large downwash flow of a V/STOL configuration out of the test region, hopefully in a manner to produce the correct downwash trajectory. The effects of varying the louver angle are shown in Fig. 10. At low values of C_μ, the wing pitching-moment coefficient appears to be favorably

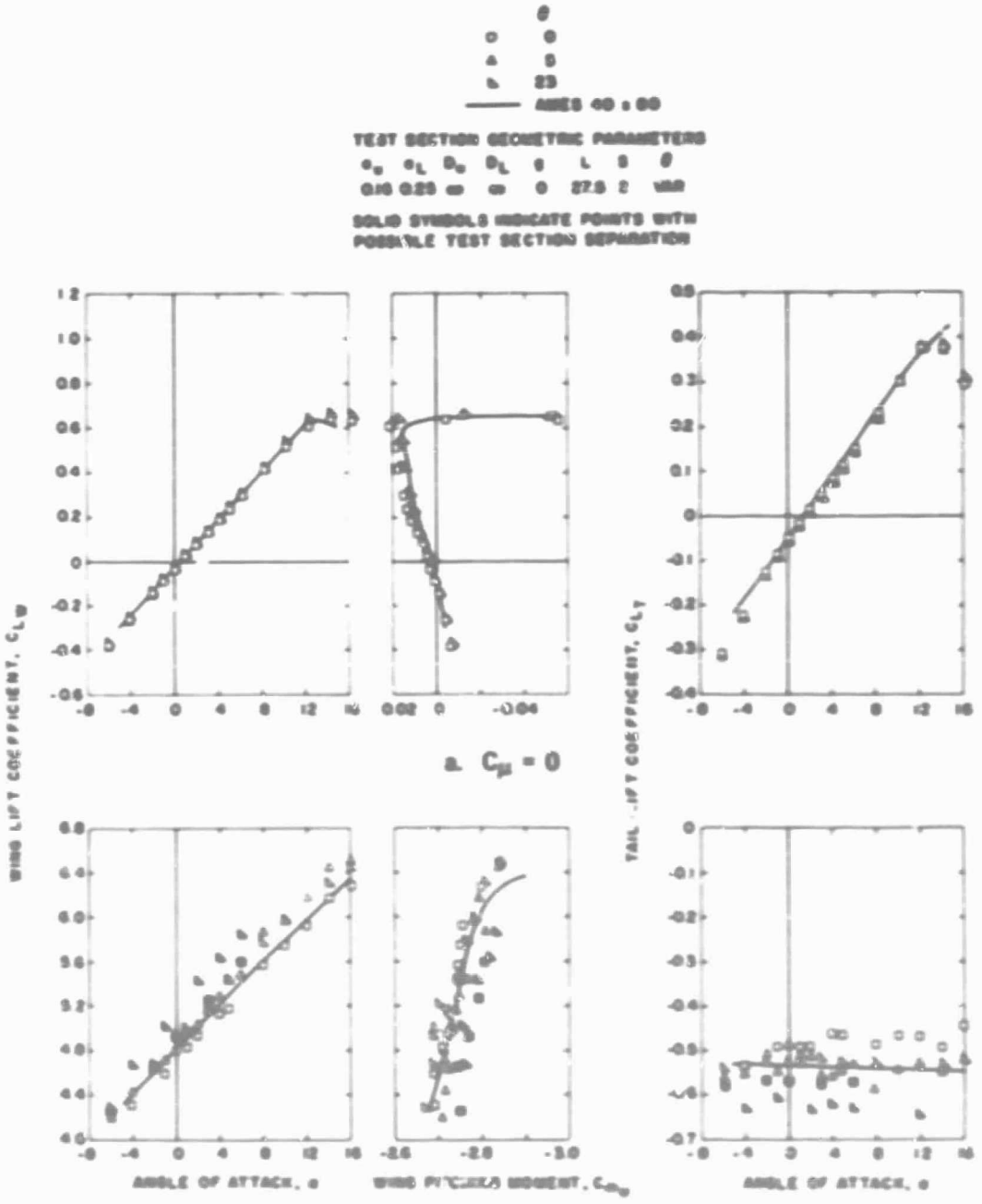

Figure 10. Effect of louver angle on the jet-flap model forces.

affected by the flow curvature induced by the louvers with the lift coefficient being essentially unaffected. The tail lift coefficient data, however, indicate a decrease in the local flow angle as louver angle is increased. At high values of C_μ there is considerable data scatter (solid symbols), particularly for θ = 23 deg. Examination of the V/STOL tunnel energy ratio for θ = 0 and 23 deg (Fig. 11) shows several points (solid symbols corresponding to those in Fig. 10) which are not along a monotonic curve. Since the energy ratio is decreased for the solid symbol points, i.e., the tunnel losses are increased, it can be inferred that there is an intermittent flow separation in the test section with this configuration. Disregarding the solid symbols, the use of louvers does not seem to have a significant advantage over the θ = 0 configurations. As the louver angle is increased, the apparent flow angle decreases and $\partial C_L/\partial\alpha$ increases indicating the louvers increase the effective solidity of the test section. The effect of louver angle on C_{m_u} and C_{L_T} is generally within the data accuracy.

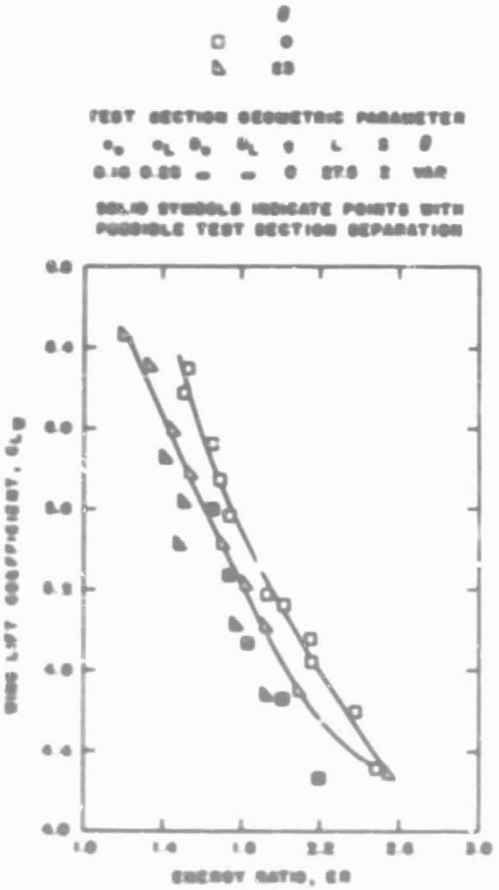

Figure 11. Effect of louver angle on the tunnel energy ratio, C_μ = 3.3.

The effect of slots in the top and bottom-stepped wall is presented in Figs. 12 and 13, respectively. Tuft studies show that slots about an inch wide are needed to prevent separation on the top wall at high values of C_μ. Slots in the top wall have more influence

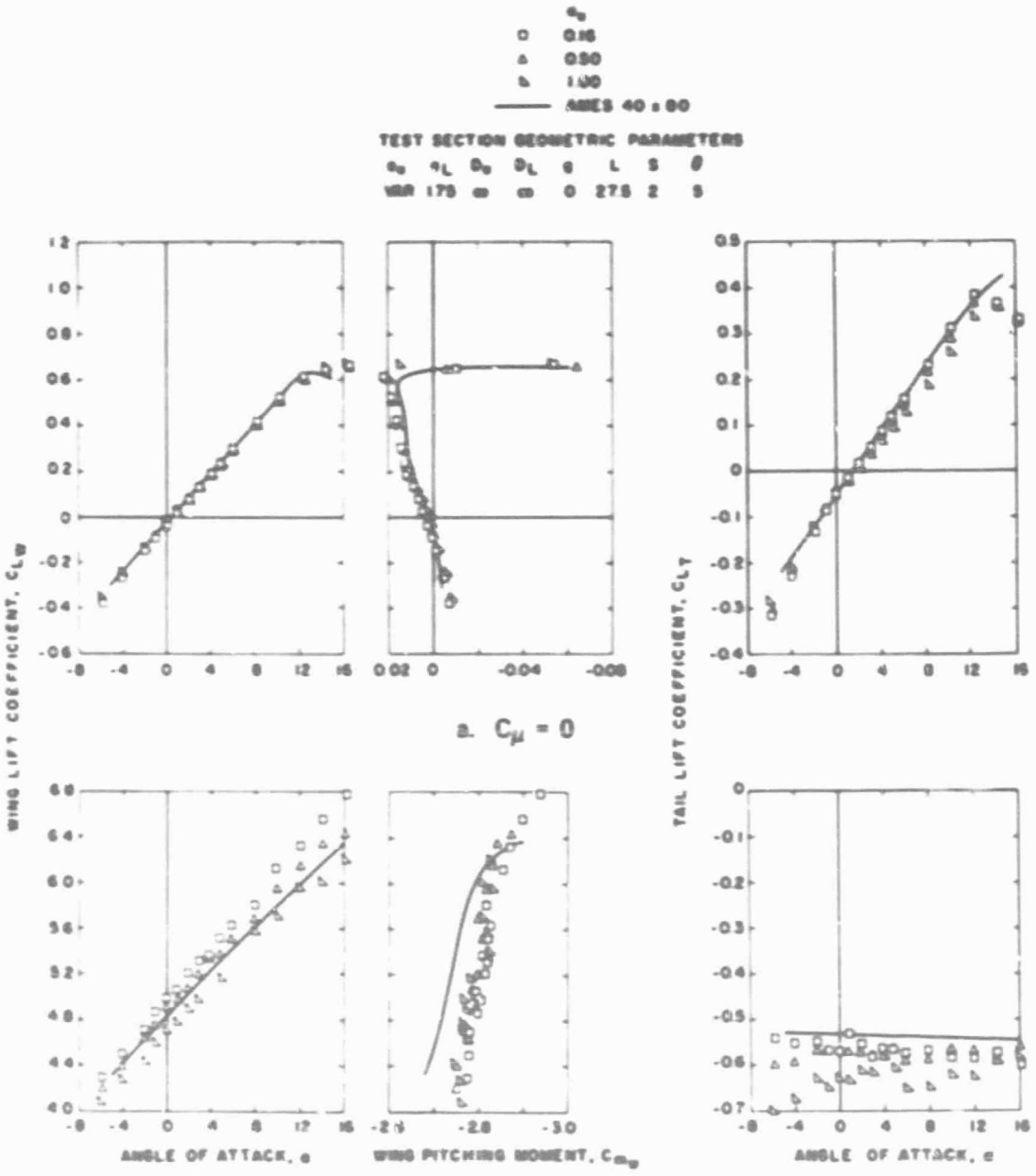

a. $C_\mu = 0$

b. $C_\mu = 3.3$

Figure 12. Effect of top wall slots on the jet-flap model forces.

on C_{L_w} and C_{L_T} than those in the stepped bottom wall. Apparently, the thick boundary layer along the bottom wall renders the slots somewhat ineffective. Although, as shown, the wing pitching moment tends to approach the interference free value as the slot width is increased, the data from the V/STOL tunnel are not quite in agreement with the Ames results.

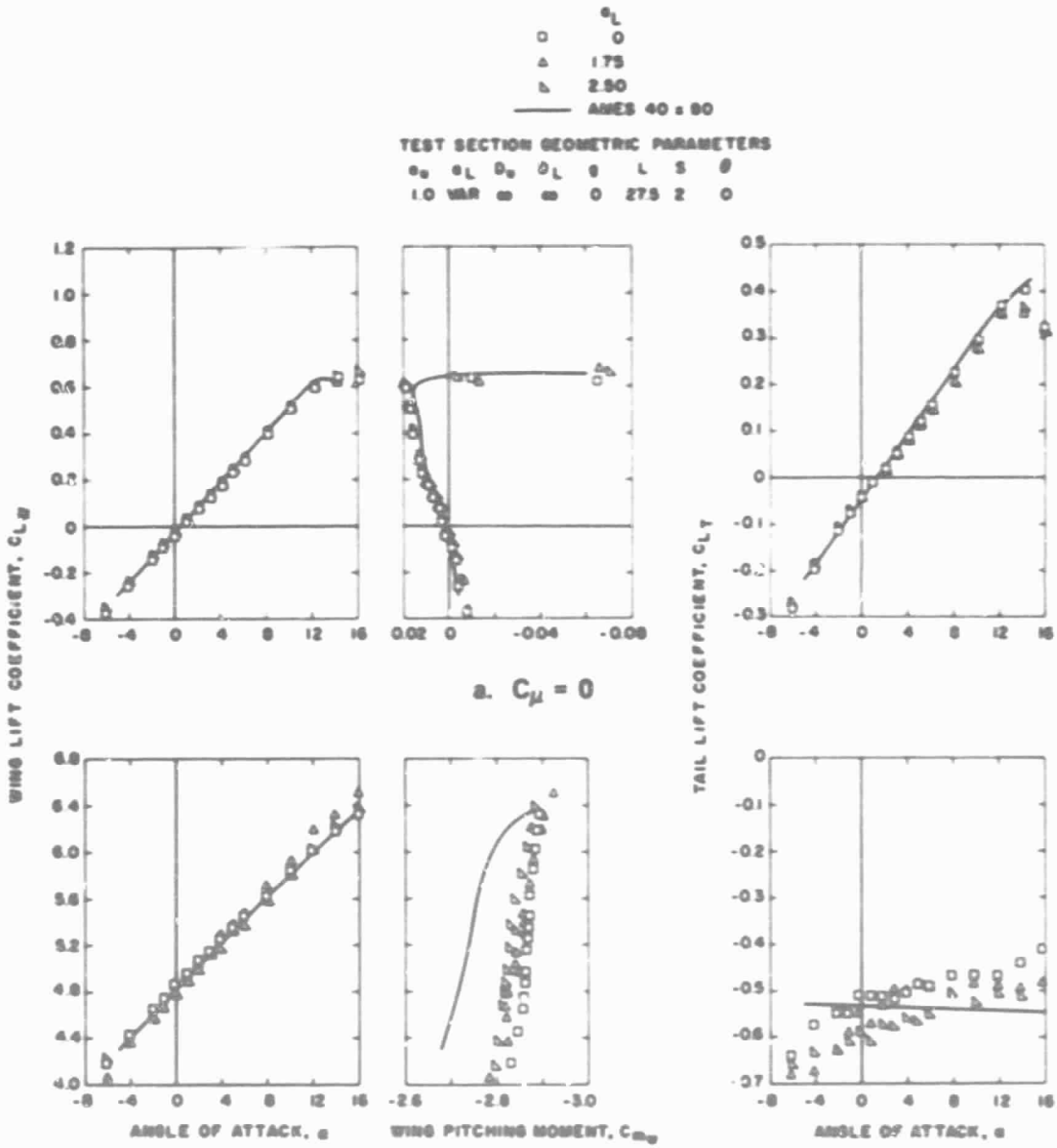

a. $C_\mu = 0$

b. $C_\mu = 3.3$

Figure 13. Effect of bottom wall slots on the jet-flap model forces.

While the slotted bottom wall was being tested, three configurations with reduced plenum depth were also investigated, as shown in Fig. 14. As might be expected, reducing the plenum depth caused the bottom wall to act more closed on the basis of C_{L_w}. It is curious that the wing pitching moment at C_μ = 3.3 is about the same for D_L of 4

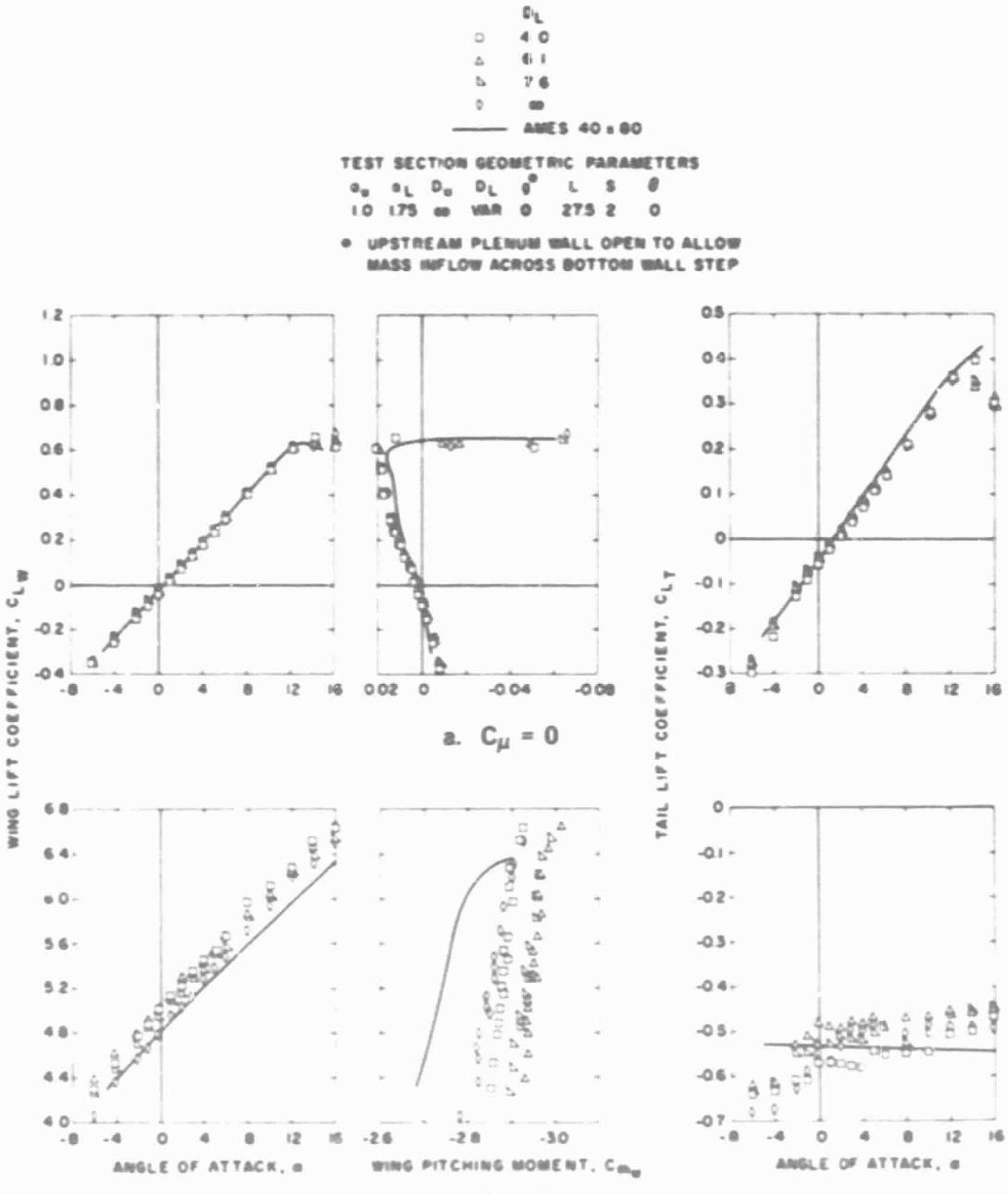

Figure 14. Effect of the bottom wall plenum depth on the jet-flap model forces.

in. and infinity. The only effect of reducing the top wall plenum depth from infinity to 2 in. (Fig. 15) is to induce an apparent flow angularity into the tunnel. The flow angularity, however, is a function of C_μ (note the C_{L_w} versus α curves shift in opposite directions for C_μ of zero and 3.3). While the effect of the top plenum depth is rather small, a depth somewhat greater than 2 in. (in the V/STOL tunnel scale) seems warranted.

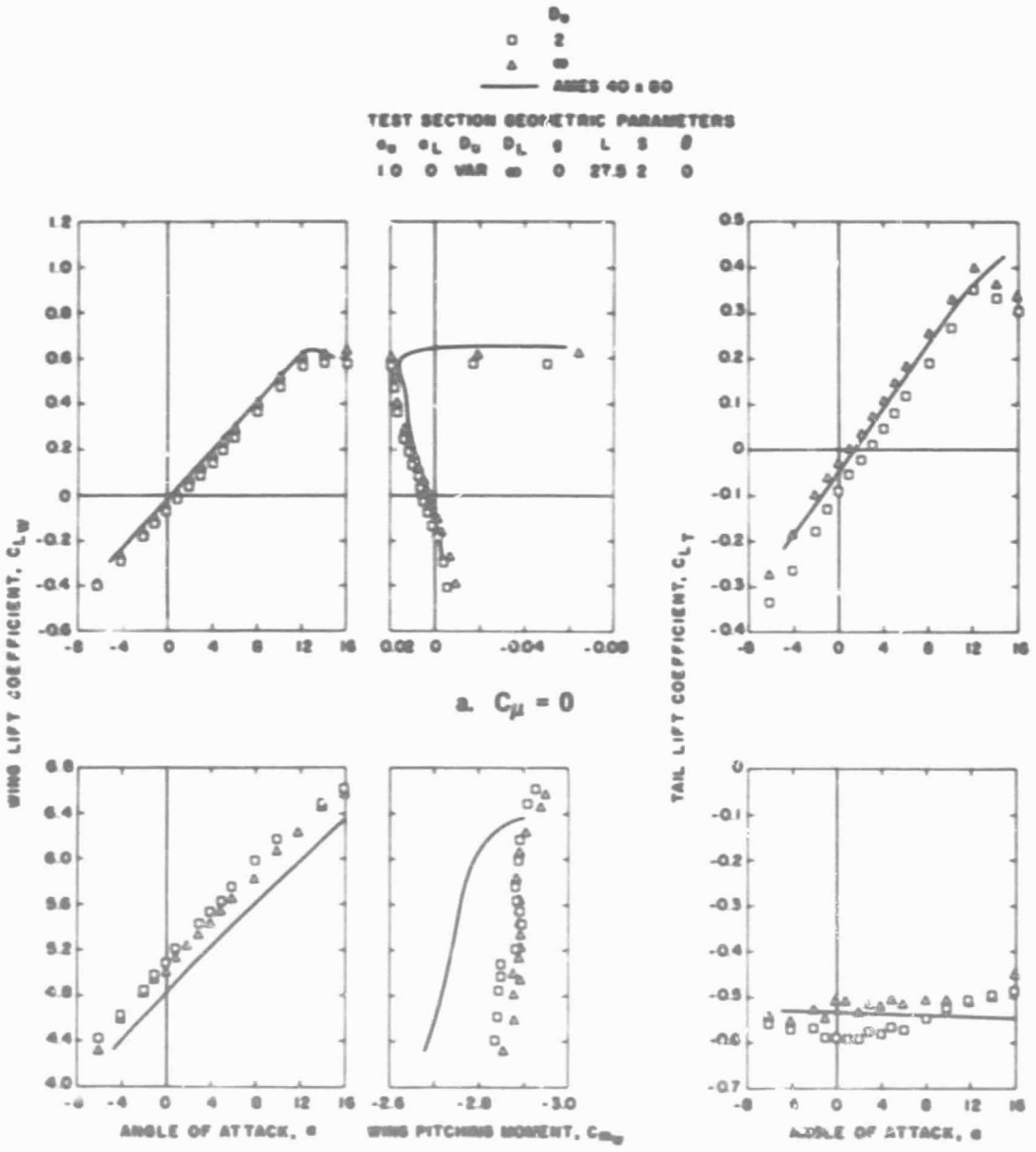

Figure 15. Effect of the top wall plenum depth on the jet-flap model forces.

All of the configurations discussed heretofore were structured such that flow from the infinite plenum could pass through the step in the bottom wall. It was found to be essential that flow pass through the step to produce near interference-free data. The amount of flow is controlled by the ejector action of the tunnel/model stream. Rather than construct a plenum in the bottom wall to provide the required flow by leakage/recirculation, a transverse slot was introduced in the bottom wall at the nozzle exit to provide the required bleed flow. The effect of the small but unknown flow through the step, which is proportional to the transverse slot width, is shown in Fig. 16. At low

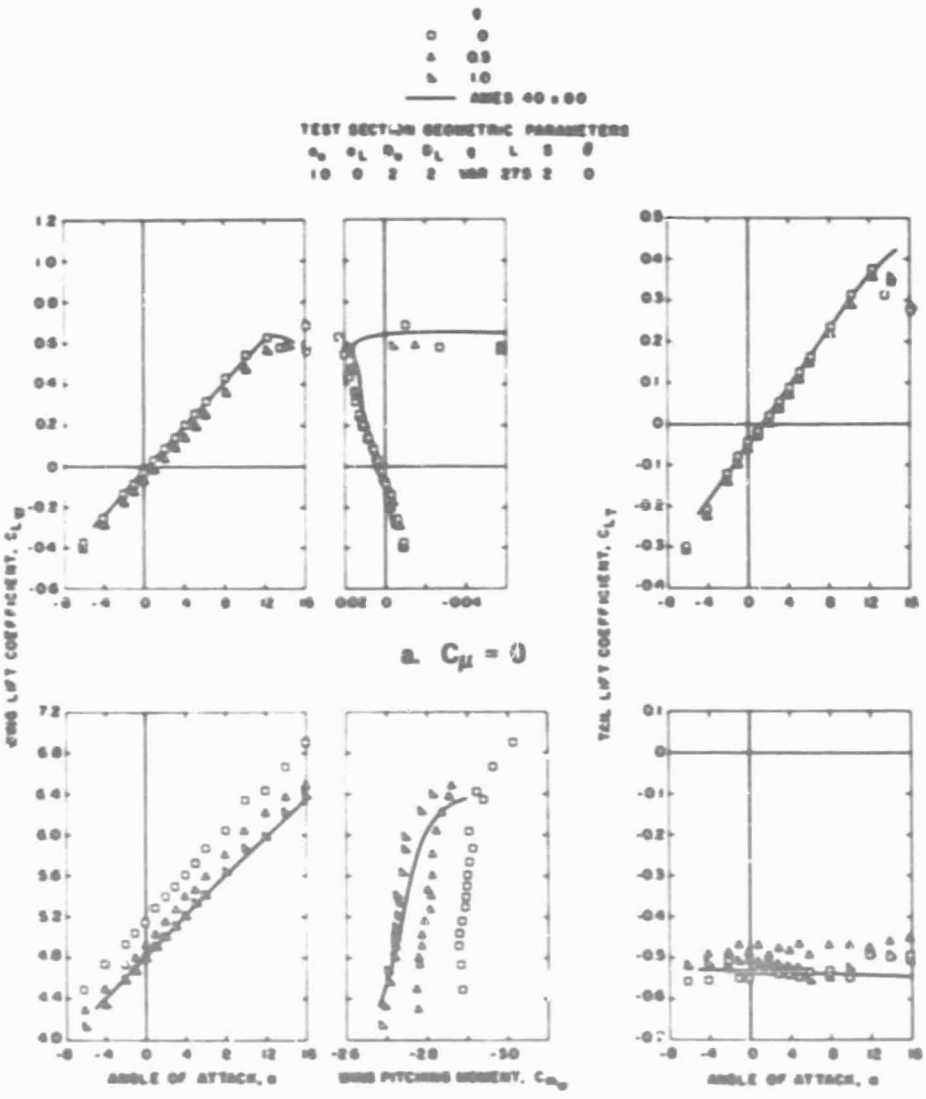

a. $C_\mu = 0$

b. $C_\mu = 3.3$

Figure 16. Effect of the bottom wall transverse slot on the jet-flap model forces.

values of C_μ, the flow through the step introduces an apparent flow angle of 0.6 deg at both the wing and tail positions. However, $\partial C_{L_w}/\partial\alpha$ and C_{L_w} versus C_m are in very good agreement with the Ames data. At higher values of C_μ the proper flow through the step results in reasonable agreement of all three force coefficients with the interference-free data. It should be noted that the 1-in. transverse slot width apparently provides the same flow through the step as the infinite plenum. Therefore, there is no need to make the slot larger. Further, the configurations with $a_\mu = 1.0$, $a_L = 0$, $D_w = 2$, $L = 2.75$, $s = 2$, $\theta = 0$ and either $g = 1$, $D_L = 2$ or $g = 0$, $D_L = \infty$ were the only configurations which were found to provide reasonable agreement between the V/STOL tunnel and Ames tunnel data for all values of C_μ. Although the data obtained in the V/STOL tunnel are not in perfect agreement with the interference-free results, comparison of the data of Figs. 16b and 7b indicates that the best stepped configuration produces much better results than a conventional test section configuration for the V/STOL case.

4.3 EVALUATION OF THE STEPPED WALL CONFIGURATION WITH THE JET-IN-FUSELAGE MODEL

Tests were also conducted with the jet-in-fuselage model and the test section configuration which produced the best results with the jet-flap model. The lift data from the configuration presented in Fig. 17 (square symbols) indicate an apparent flow angularity

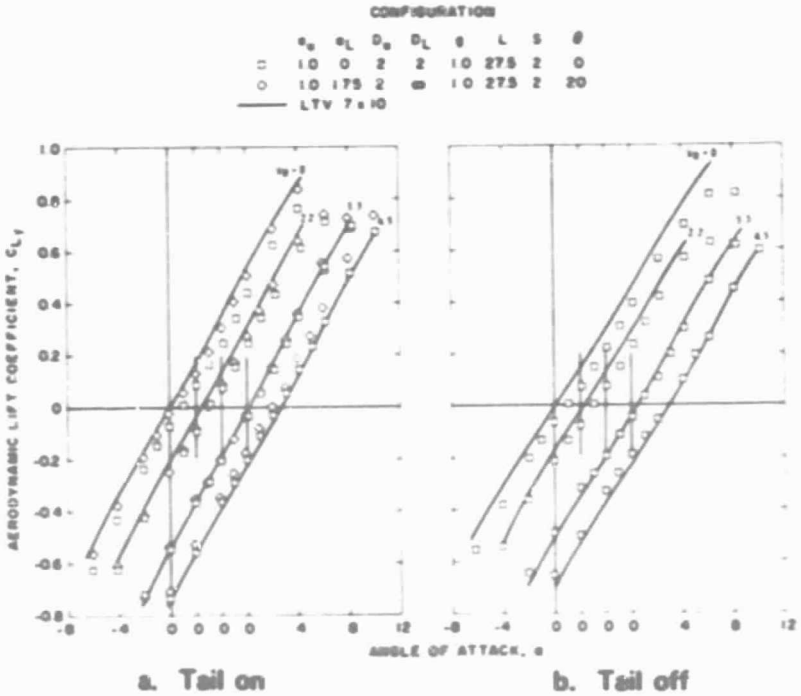

a. Tail on b. Tail off

Figure 17. Effect of the stepped bottom wall configurations on the jet-in-fuselage model lift.

similar to that experienced by the jet-flap. $\partial C_L/\partial\alpha$ is essentially the same as the interference-free results. However, the pitching moment, Fig. 18, is significantly less than the interference-free results. Tufts indicated tunnel flow breakdown had occurred at V_R = 4.5 with flow moving upstream along the floor ahead of the jet/wall intersection and vertically along the sidewalls. It could be inferred from the C_{m_f} data that flow breakdown was also present to some extent at the lower velocity ratios.

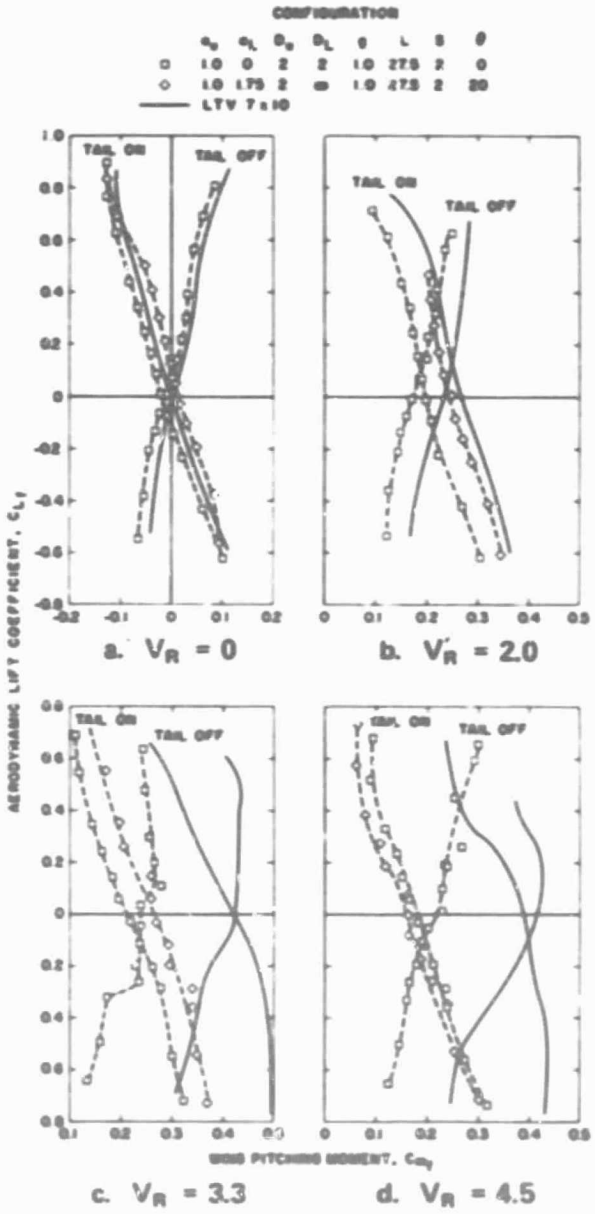

Figure 18. Effect of the stepped bottom wall configuration on the jet-in-fuselage model pitching moment.

Additional tests were conducted with the louvers open and the bottom wall plenum removed. The data, also presented in Figs. 17 and 18 (diamond symbols), show the same effects observed with the jet-flap model. The apparent flow angle is less at all values of V_R. $C_{L_f}/\partial\alpha$ increased indicating an effectively lower wall porosity than with the louvers closed. However, the pitching moment was appreciably affected, except at $V_R = 4.5$, in contrast to the jet-flap configuration.

5.0 CONCLUDING REMARKS

The investigation of wind tunnel wall interference for V/STOL models reported herein and in Ref. 4 has shown that agreement between theory and experiment hinges upon the theoretical representation of the boundary condition. Kraft's heuristic modification to the boundary condition, while producing better agreement with experiment, is not sufficiently descriptive of the physical process to lead to an understanding of the mechanism of the jet (downwash)/boundary interaction.

It has been demonstrated in the present investigation that at least one test section configuration exists for a jet-flap model which will reasonably represent free-air flow conditions over a wide range of jet momentum coefficient. The configuration is not suitable for a high-disc-loading model, however. The possibility certainly exists that the results with the jet-flap model are fortuitous. The results of Ref. 4 and the present study indicate many wall configurations will result in free-air C_L versus α data, but few will produce free-air pitching moment with augmented lift. The primary difficulty in attaining an interference-free field is apparently associated with the model downwash/tunnel boundary interaction. The effect of various wall geometries, however simple or complicated, cannot be understood until a better understanding of the boundary phenomena is attained. Until that time, there seems little likelihood that any interference-free tunnel configuration could be used with confidence. It is felt, therefore, that future work on V/STOL wind tunnel wall interference (both theoretical and experimental) should be directed toward understanding the tunnel boundary condition.

REFERENCES

1. Theodorsen, Theodore. "The Theory of Wind-Tunnel Wall Interference." NACA Report 410, 1932.

2. Wright, Ray H. and Ward, Vernon G. "NACA Transonic Wind Tunnel Test Sections." NACA Report 1231, 1955.

3. Goethert, Bernhard H. Transonic Wind Tunnel Testing. Pergamon Press, New York, 1961.

4. Binion, T. W., Jr. "An Investigation of Several Slotted Wind Tunnel Wall Configurations with a High Disc Loading V/STOL Model." AEDC-TR-71-77 (AD723294), May 1971.

5. Lazzeroni, F. A. and Carr, L. W. "Problems Associated with Wind Tunnel Tests of High-Disc-Loading Systems and Low Forward Speeds." Proceedings of the Third CAL/AVLABS Symposium, Aerodynamics of Rotary Wing and V/STOL Aircraft, Vol. II, Wind Tunnel Testing. The U.S. Army Aviation Material Laboratories and Cornell Aeronautical Laboratory, Inc., Buffalo, New York, June 18-20, 1969.

6. Anonymous. "Ames Research Facilities Summary." NASA/Ames Research Center, 1974.

7. Holbrook, J. W. "Low Speed Wind Tunnel Handbook." Ling-Temco-Vought Publication No. AER-EOR 12995-A, Dallas, Texas, March 1965.

8. Binion, T. W., Jr. "Description and Calibration of the AEDC Low Speed Wind Tunnel (V/STOL). "AEDC-TR-70-266 (AD877999), December 1970.

9. Gurdley, Gottfried. "Simplifications of the Boundary Conditions at a Wind Tunnel Wall with Longitudinal Slots." WADC-TR-53-150, April 1953.

10. Chen, C. F. and Mears, J. W. "Experimental and Theoretical Study of Mean Boundary Conditions at Perforated and Longitudinally Slotted Wind Tunnel Walls." AEDC-TR-57-20 (AD144320), December 1957.

11. Kraft, E. M. "Analytical Study of Ventilated Wind Tunnel Boundary Interference on V/STOL Models Including Wake Curvature and Decay Effects." AEDC-TR-74-51 (ADA000922), November 1974.

12. Heyson, Harry H. "Linearized Theory of Wind Tunnel Jet-Boundary Corrections and Ground Effect for VTOL-STOL Aircraft." NASA TR R-124, 1962.

13. Lo, Ching-Fang. "Wind-Tunnel Boundary Interference on a V/STOL Model." Journal of Aircraft, Vol. 8, No. 3, March 1971, pp. 162-167.

14. Kraft, E. M. "Upwash Interference on a Symmetrical Wing in a Retangular Ventilated Wall Wind Tunnel: Part I - Development of Theory." AEDC-TR-72-187 (AD757196), March 1973.

NOMENCLATURE

a	Slot width, in.
b	Test section semiheight, in.
C	Tunnel cross-sectional area, sq in.
C_{L_f}	Aerodynamic lift coefficient of jet-in-fuselage model
C_{L_T}	Tail lift coefficient
C_{L_w}	Wing lift coefficient of jet-flap model
C_{m_f}	Aerodynamic pitching moment of jet-in-fuselage model
C_{m_w}	Wing pitching moment of jet-flap model
C_μ	Jet momentum coefficient, $m_j V_j / q_\infty s$
$\bar{c}$	Mean aerodynamic chord, in.
D	Plenum depth, in.
d	Slat width, in.
ER	Tunnel energy ratio, dynamic pressure divided by the pressure rise across the fan
g	Transverse slot width, in.
h	Test section semiheight, in.
k	Geometric slot parameter
L	Distance from nozzle exit to bottom wall step, in.
ℓ	Slot spacing, in. (see Eq. (3))
m_j	Model jet mass flow, slugs/sec
n	Normal direction
P	Slot parameter, $(1 + k/h)^{-1}$
q	Dynamic pressure

R	Porosity parameter
S	Step height, in.
s	Wing area, sq in.
u	Axial velocity
V_e	Effective crossflow velocity at the homogeneous test section boundary
V_j	Model jet exit velocity, ft/sec
V_R	Jet to free-stream velocity ratio, V_j/V_∞
x, y, z	Cartesian coordinates
α	Model angle of attack, deg
α_o	Angle of attack at zero lift, rad
$\Delta\alpha_j$	Jet interference angle, deg
δ_o	Upwash interference factor at the wing quarter chord
δ_u	Interference factor for the axial interference velocity
δ_w	Interference factor for the vertical interference velocity
θ	Bottom wall louver angle, deg
ϕ	Velocity potential

SUBSCRIPTS

u	Upper wall
L	Bottom wall
∞	Free-stream conditions